Supporting Information

Amine-assisted synthesis of Ni_3Fe alloy encapsulated in nitrogen-doped carbon for high-performance water splitting

Mengzhi Guo,[a] Hong Meng, *[b] Junsu Jin,[a] and Jianguo Mi*[a]

[a] *State Key Laboratory of Organic-Inorganic Composites, Beijing University of Chemical Technology, Beijing 100029, China*

[b] *State Key Laboratory of Chemistry and Utilization of Carbon Based Energy Resources, College of Chemistry, Xinjiang University, Urumqi, 830046, China*

* Corresponding author, E-mail address: menghong@mail.buct.edu.cn;

mijg@mail.buct.edu.cn

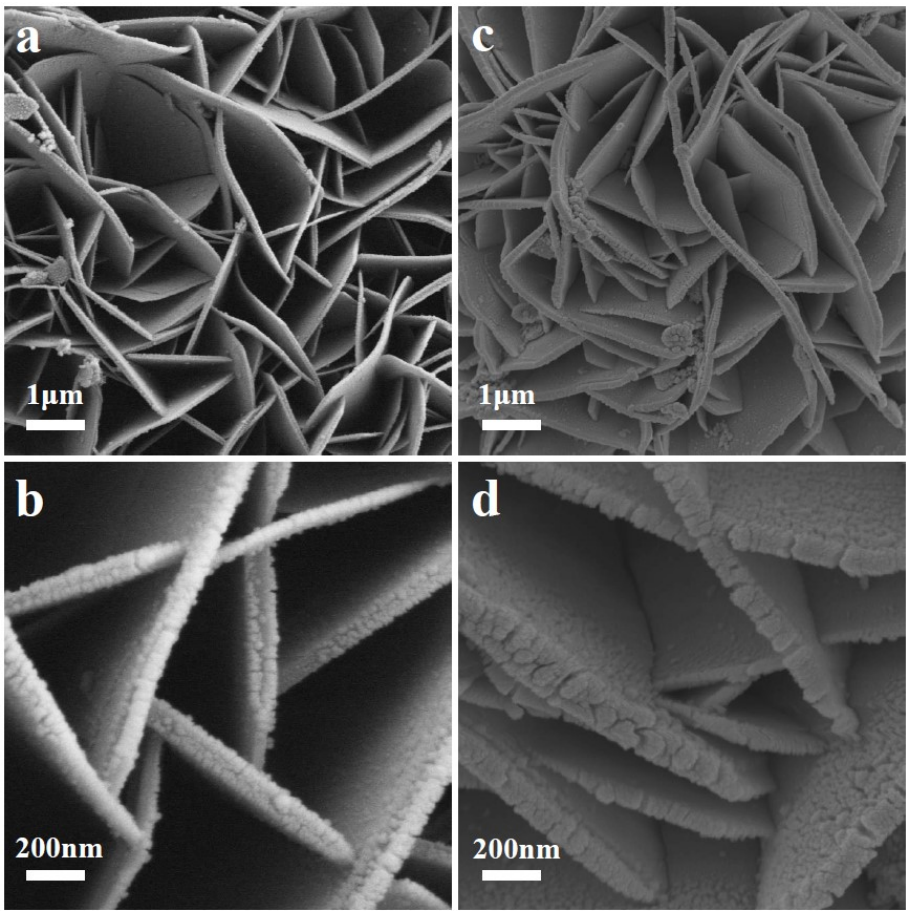

Fig. S1 SEM images of (a, b) NiFe-LDH/NF; (c, d) NiFeOx/NF.

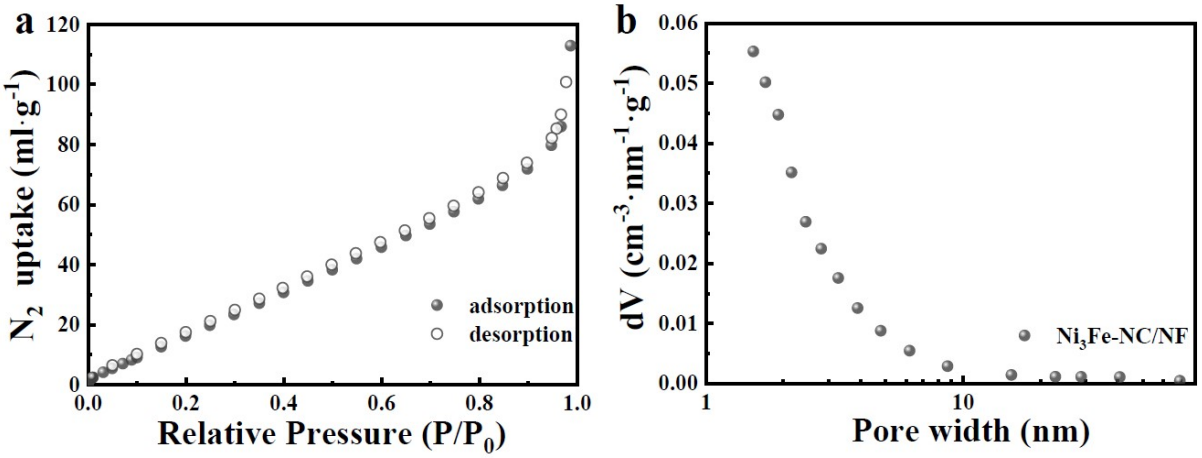

Fig. S2 (a)N_2 adsorption-desorption isotherm at 77 K and (b) pore size distribution of Ni_3Fe-NC/NF based on BJH method.

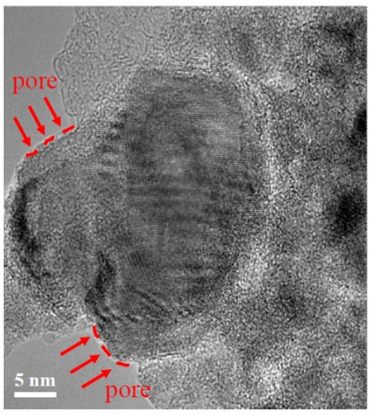

Fig. S3 TEM image of Ni_3Fe-NC/NF.

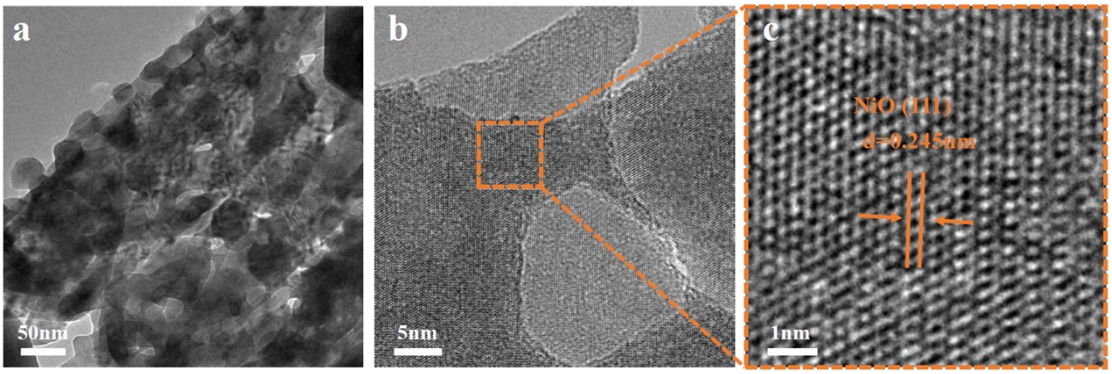

Fig. S4 (a) TEM image; (b, c) HRTEM images of NiFeOx/NF.

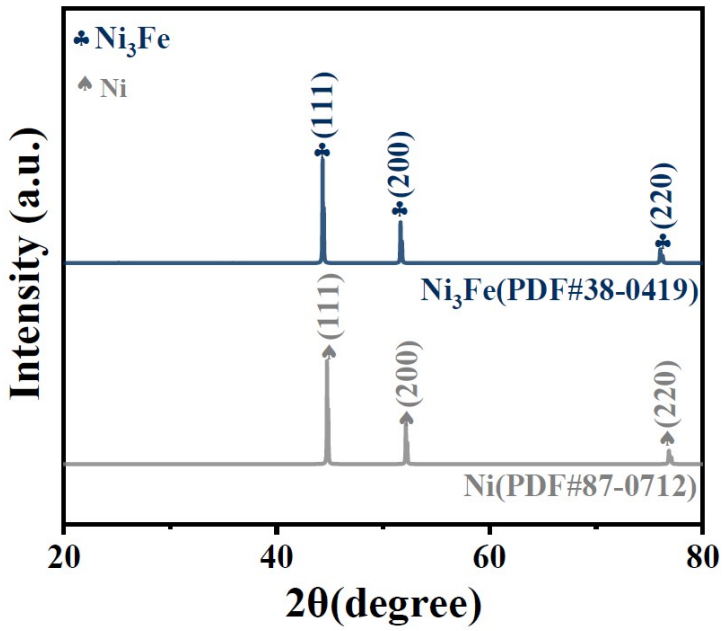

Fig. S5 XRD patterns of Ni_3Fe and Ni foam (NF).

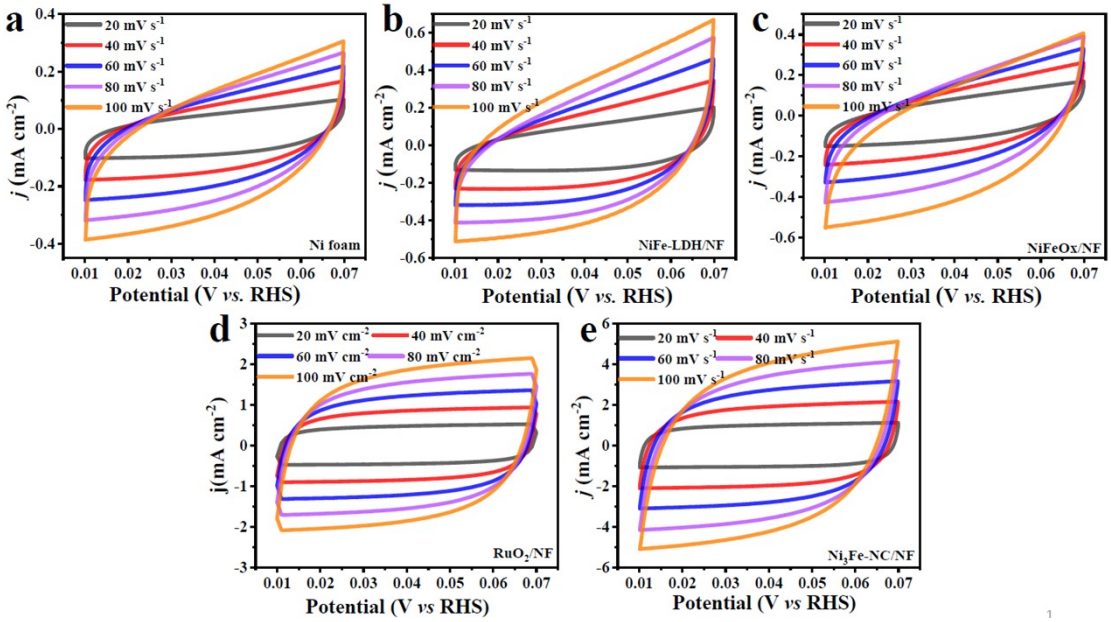

Fig. S6 CV curves of (a) NF, (b) NiFe-LDH/NF, (c) NiFeOx/NF, (d) RuO_2/NF, and (e) Ni_3Fe-NC/NF at various scan rates.

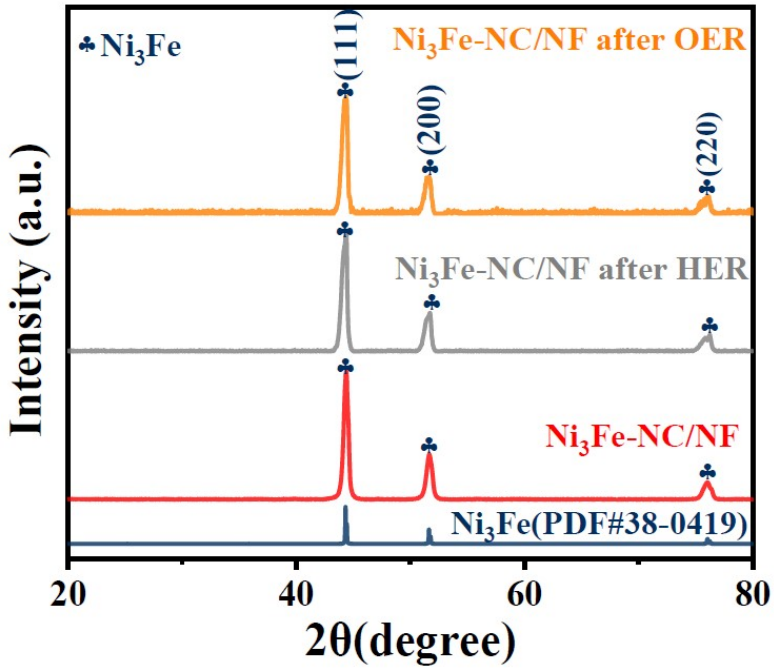

Fig. S7 XRD patterns of Ni_3Fe-NC/NF and the samples collected after OER and HER stability tests.

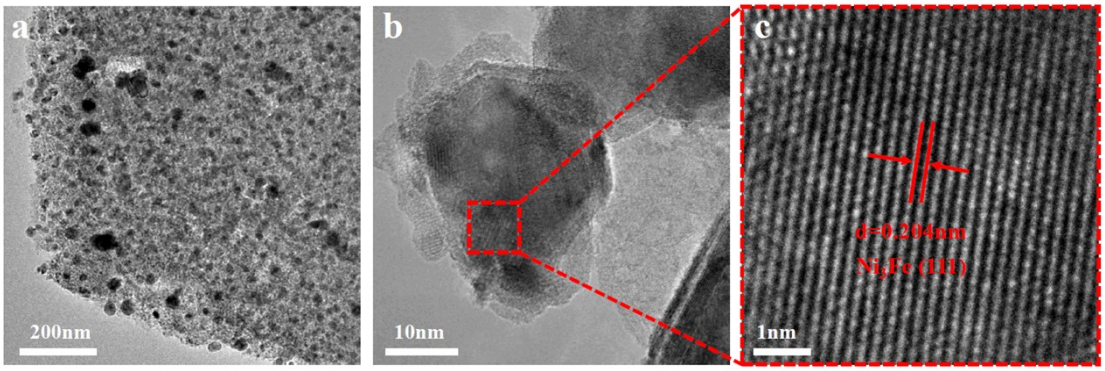

Fig. S8 (a) TEM image; (b, c) HRTEM images of Ni_3Fe-NC/NF after OER stability test.

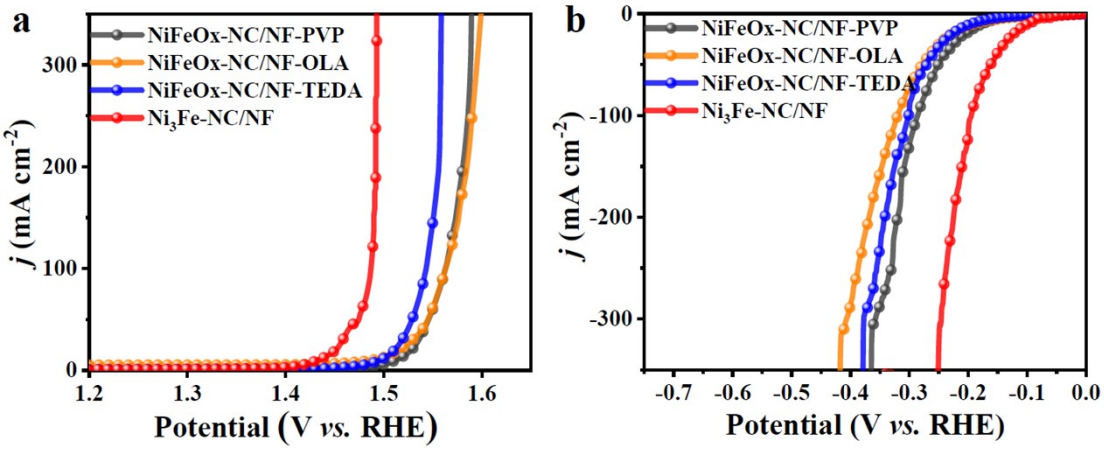

Fig. S9 OER (a) and HER (b) polarization curves of NiFeOx-NC/NF-PVP, NiFeOx-NC/NF-OLA, NiFeOx-NC/NF-TEPA, and Ni_3Fe-NC/NF in 1.0 M KOH solution with a scan rate of 5 mV s^{-1}.

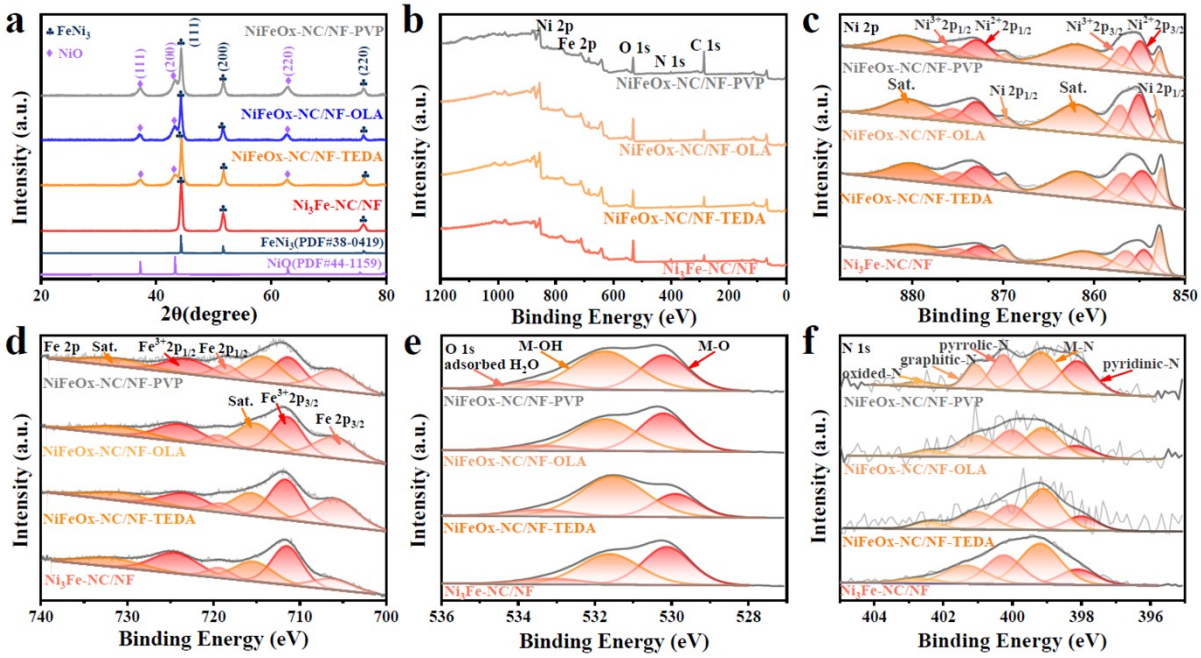

Fig. S10 Compositional characterizations of NiFeOx-NC/NF-PVP, NiFeOx-NC/NF-OLA, NiFeOx-NC/NF-TEDA, and Ni_3Fe-NC/NF. (a) XRD patterns, (b) XPS surveys, (c-f) high-resolution XPS spectra of (c) Ni 2p, (d) Fe 2p, (e) O 1s, and (f) N 1s.

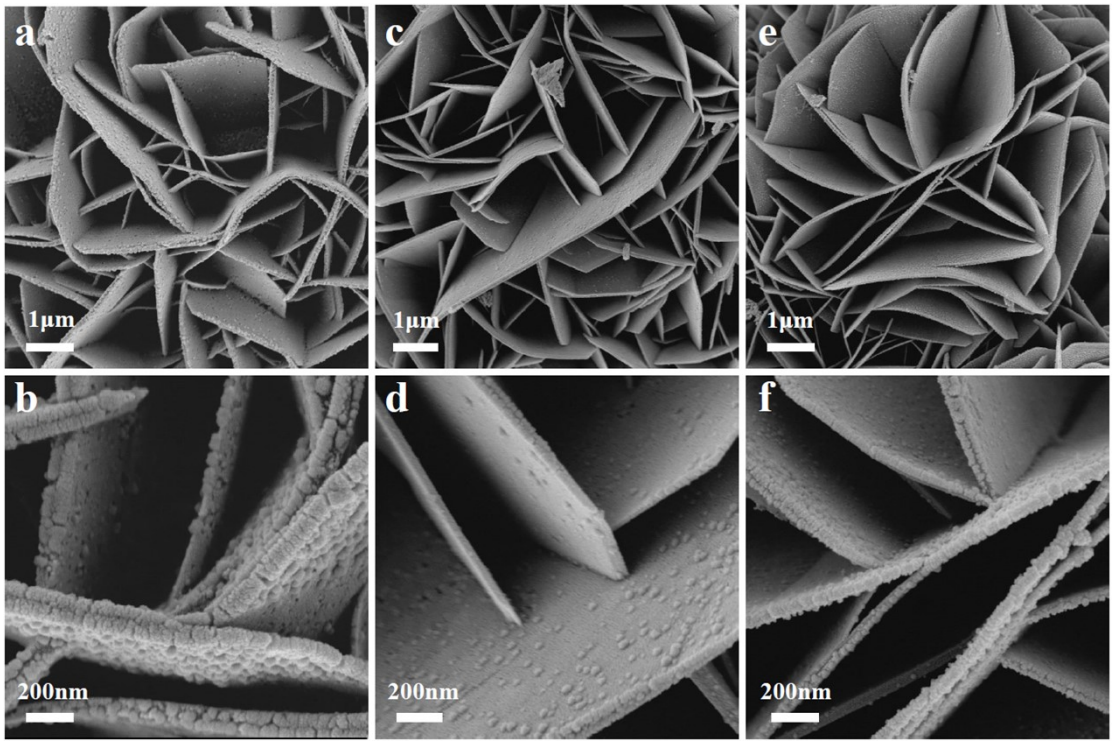

Fig. S11 SEM images of (a, b) NiFeOx-NC/NF-PVP; (c, d) NiFeOx-NC/NF-OLA; (e, f) NiFeOx-NC/NF-TEDA.

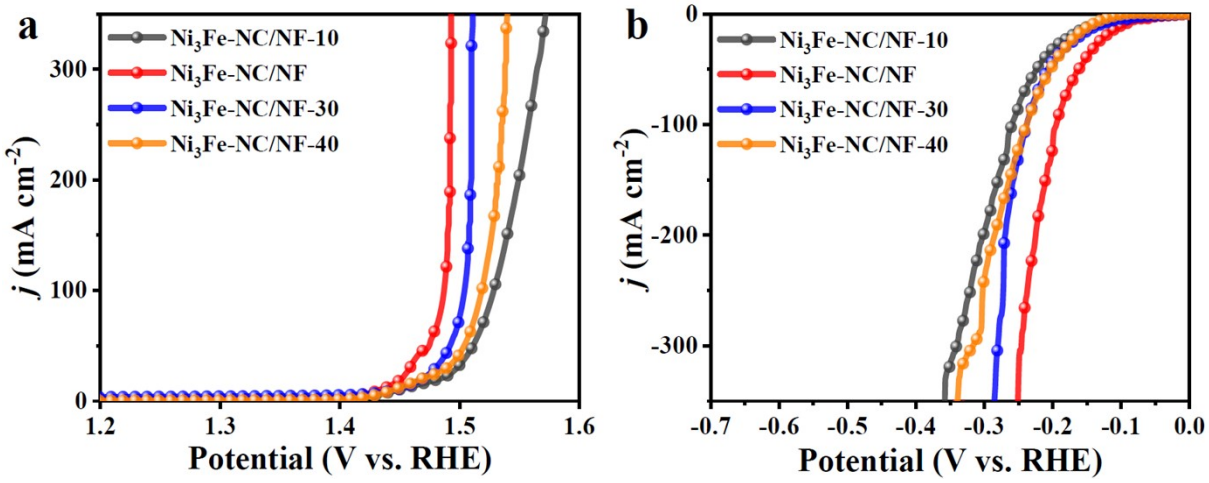

Fig. S12 OER (a) and HER (b) polarization curves of Ni_3Fe-NC/NF-10, Ni_3Fe-NC/NF-30, Ni_3Fe-NC/NF-40, and Ni_3Fe-NC/NF in 1.0 M KOH solution with a scan rate of 5 mV s^{-1}.

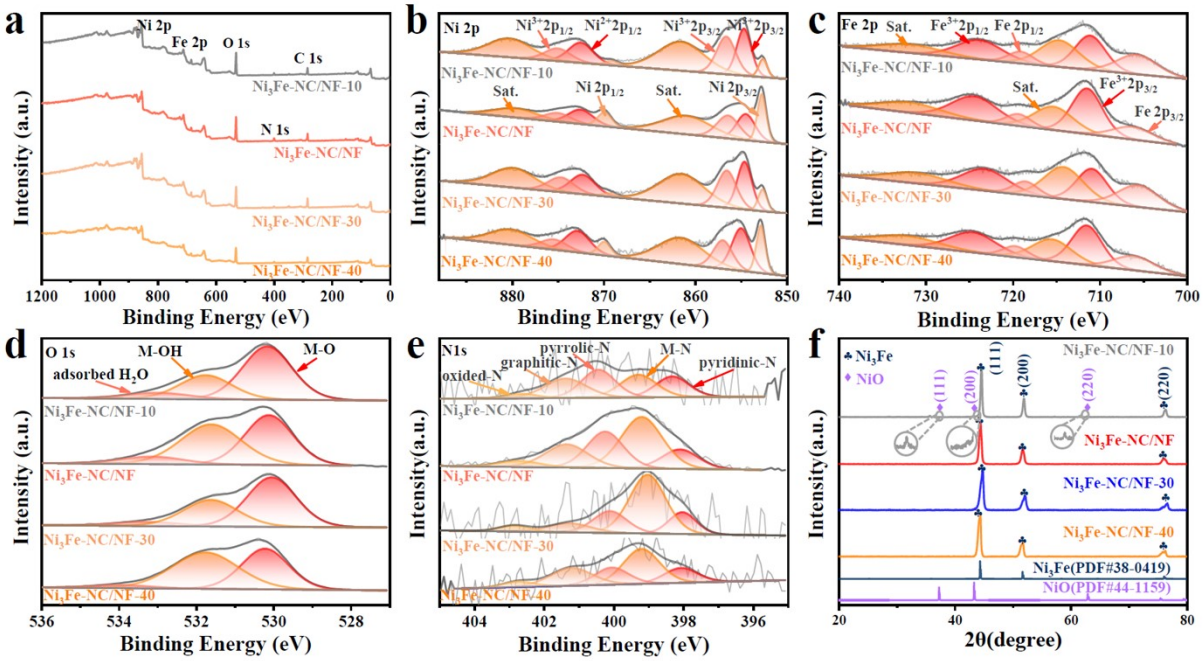

Fig. S13 Compositional characterizations of Ni_3Fe-NC/NF-10, Ni_3Fe-NC/NF, Ni_3Fe-NC/NF-30, and Ni_3Fe-NC/NF-40. (a) XPS surveys, (b-e) high-resolution XPS spectra of (b) Ni 2p, (c) Fe 2p, (d) O 1s, (e) N 1s, and (f) XRD patterns.

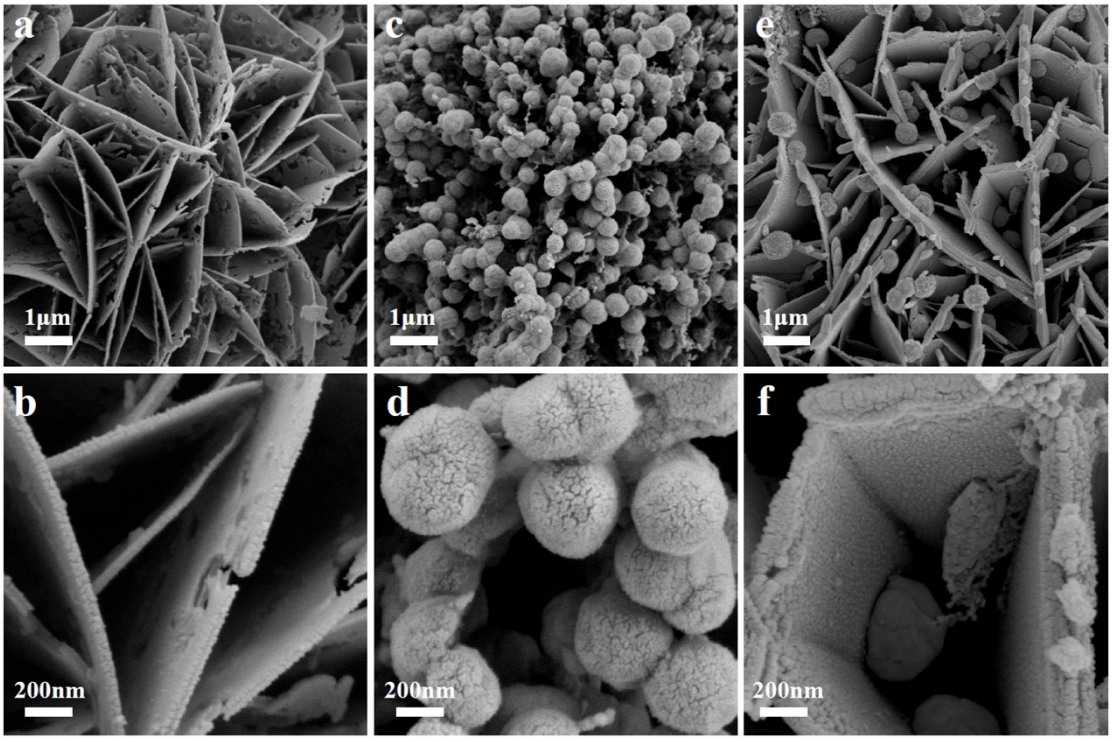

Fig. S14 SEM images of (a, b) Ni_3Fe-NC/NF-10; (c, d) Ni_3Fe-NC/NF-30; (e, f) Ni_3Fe-NC/NF-

40.

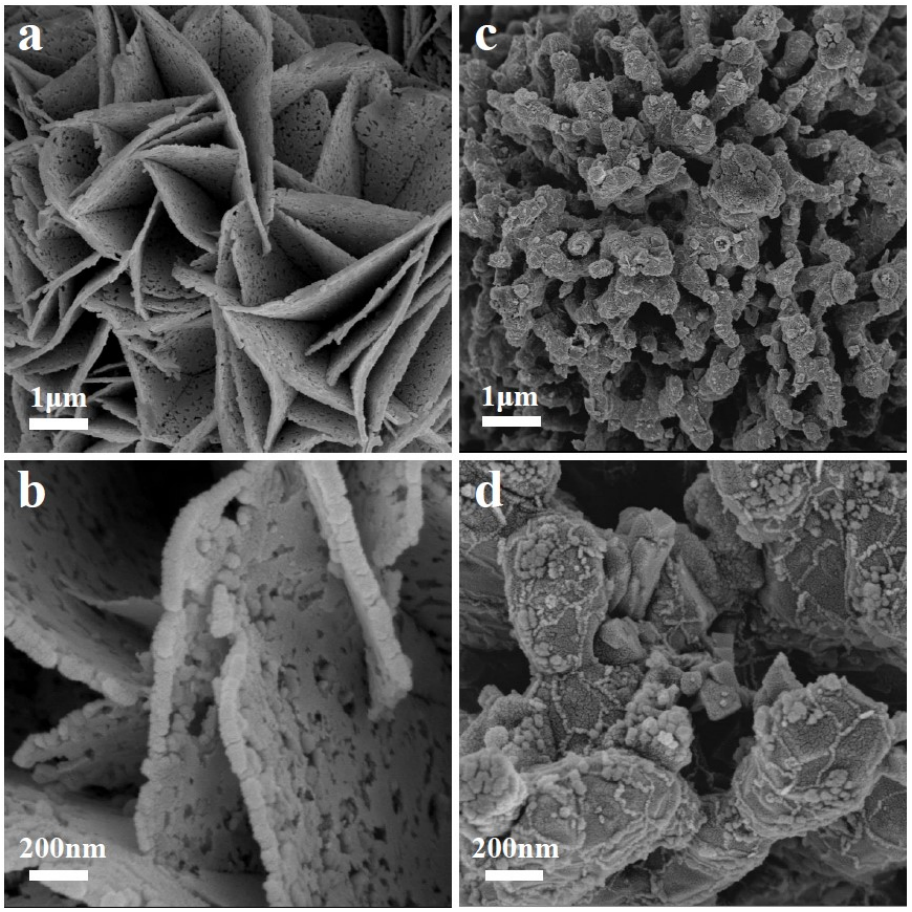

Fig. S15 SEM images of (a, b) NiFeOx-NC/NF-400; (c, d) NiFeOx-NC/NF-600.

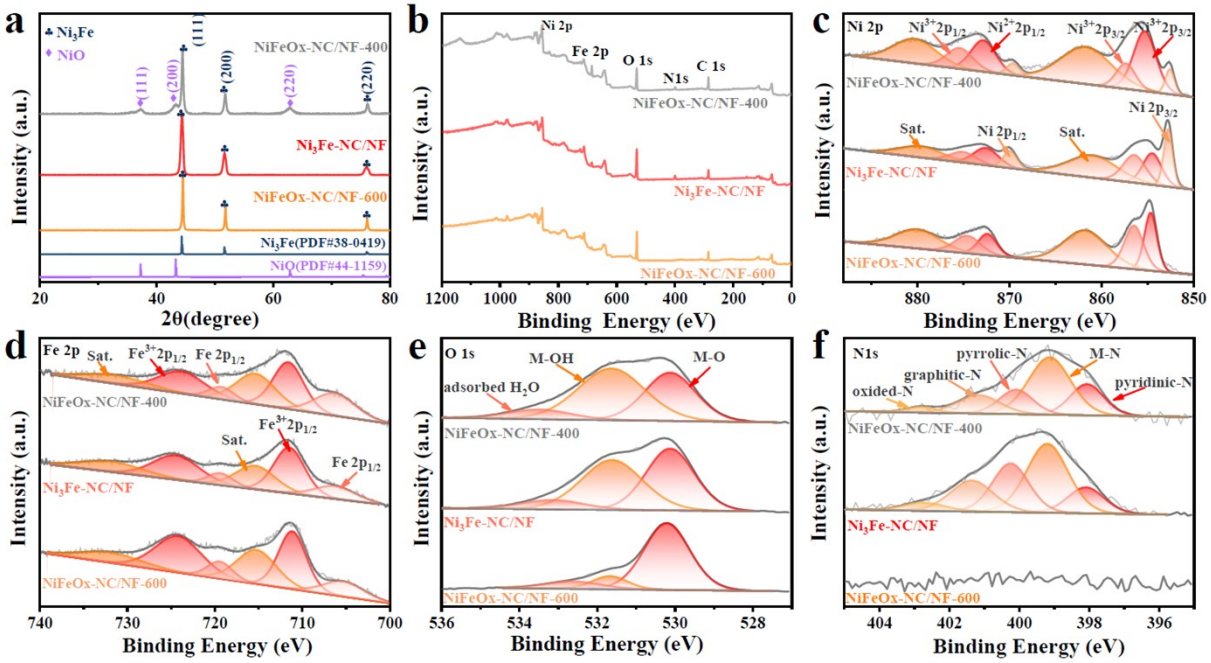

Fig. S16 Compositional characterizations of NiFeOx-NC/NF-400, Ni_3Fe-NC/NF, and NiFeOx-NC/NF-600. (a) XRD patterns, (b) XPS surveys, (c-f) high-resolution XPS spectra of (c) Ni 2p, (d) Fe 2p, (e) O 1s, and (f) N 1s.

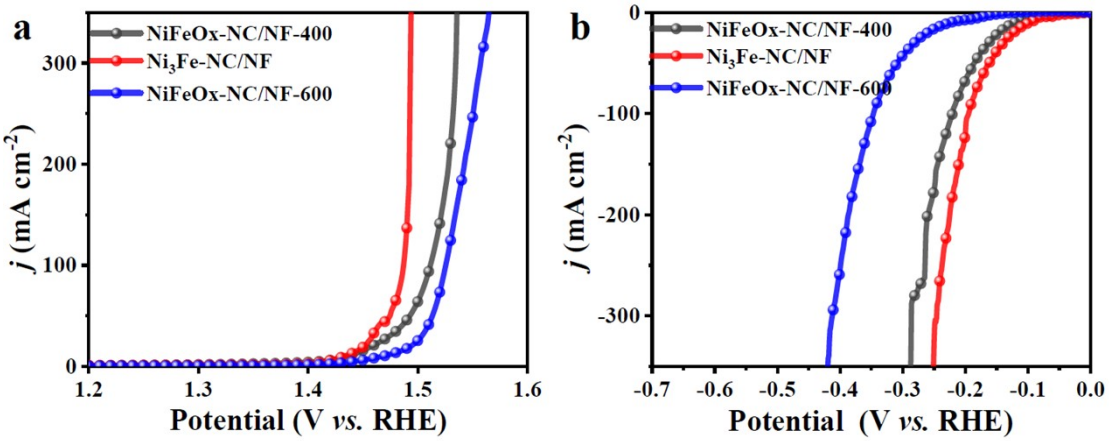

Fig. S17 OER (a) and HER (b) polarization curves of NiFeOx-NC/NF-400, Ni_3Fe-NC/NF, and NiFeOx-NC/NF-600 in 1.0 M KOH solution with a scan rate of 5 mV s^{-1}.

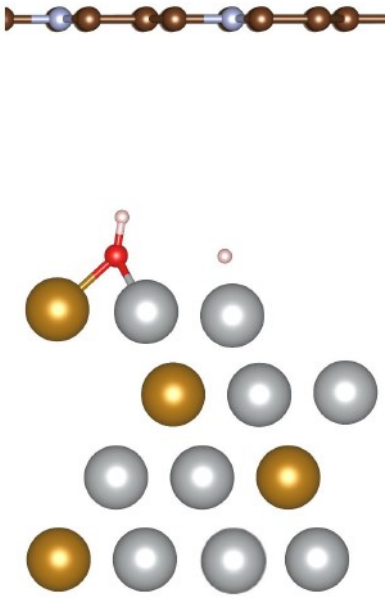

Fig. S18 The geometric structure of *H on Ni_3Fe-OH/NC.

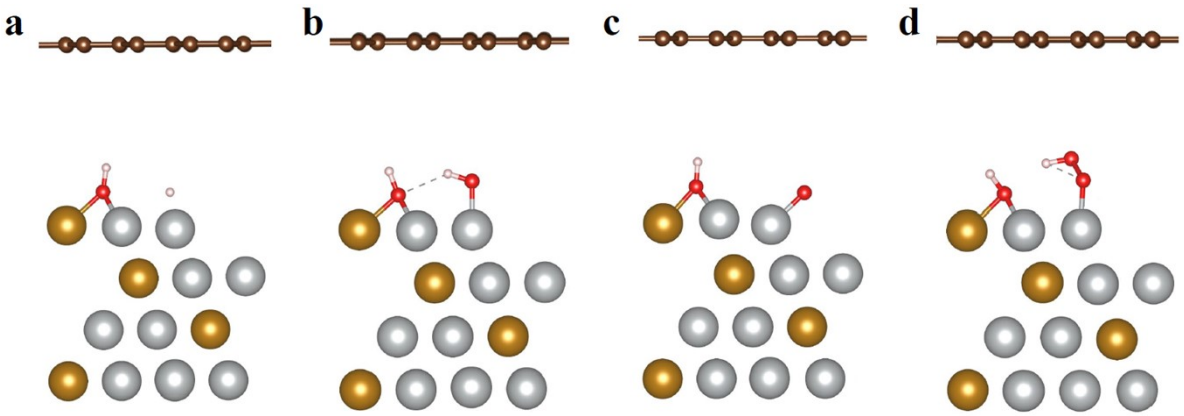

Fig. S19 The geometric structures of (a) *H, (b-c) *OH, *O, and *OOH on Ni_3Fe-OH/C.

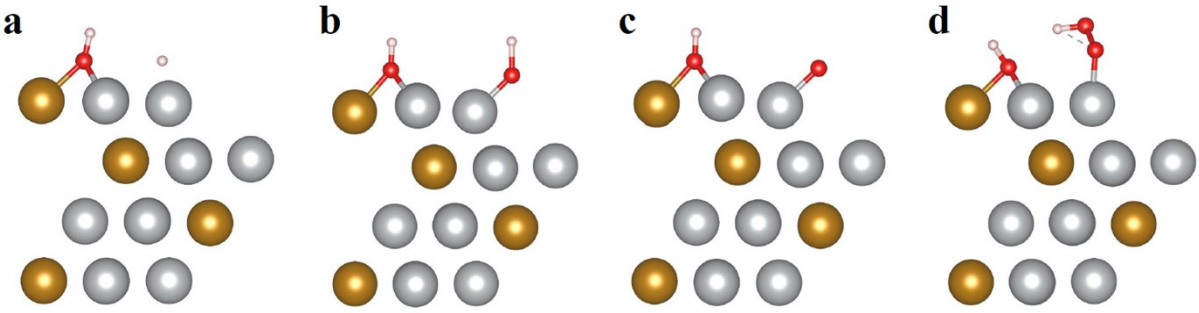

Fig. S20 The geometric structures of (a) *H, (b-c) *OH, *O, and *OOH on Ni_3Fe-OH.

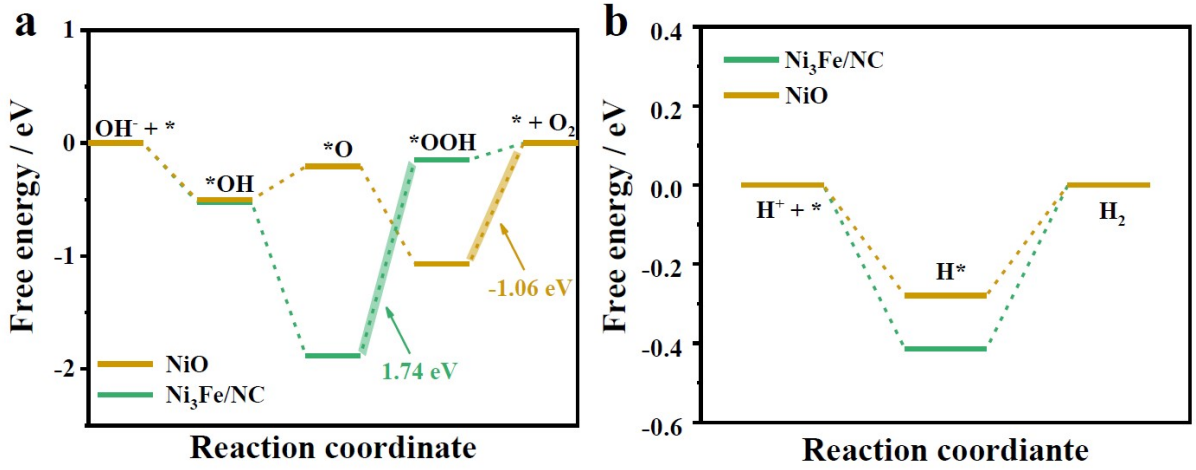

Fig. S21 (a) Gibbs free energy diagram over Ni_3Fe /NC and NiO for the OER at an equilibrium potential of 1.23 V. The highlights indicate the rate-determining step with the value of the limiting energy barrier. (b) Gibbs free energy diagram for the HER.

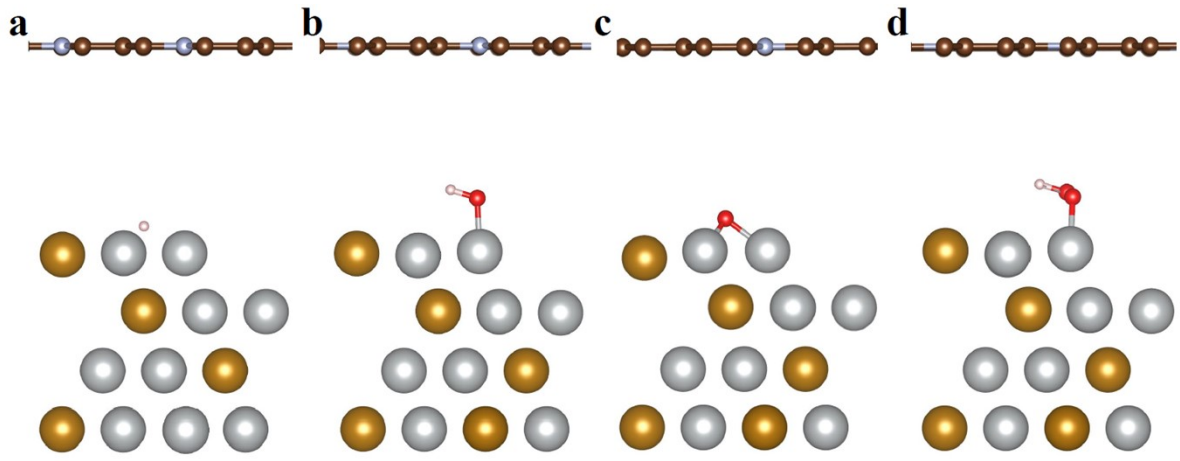

Fig. S22 The geometric structures of (a) *H, (b-c) *OH, *O and *OOH on Ni_3Fe/NC.

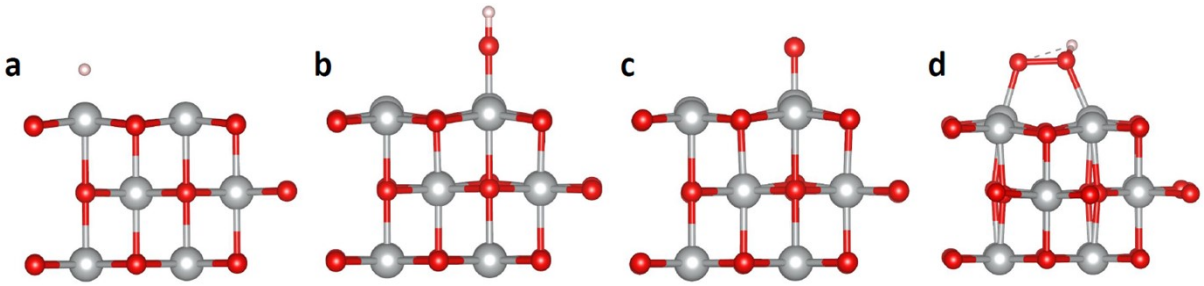

Fig. S23 The geometric structures of (a) *H, (b-c) *OH, *O and *OOH on NiO.

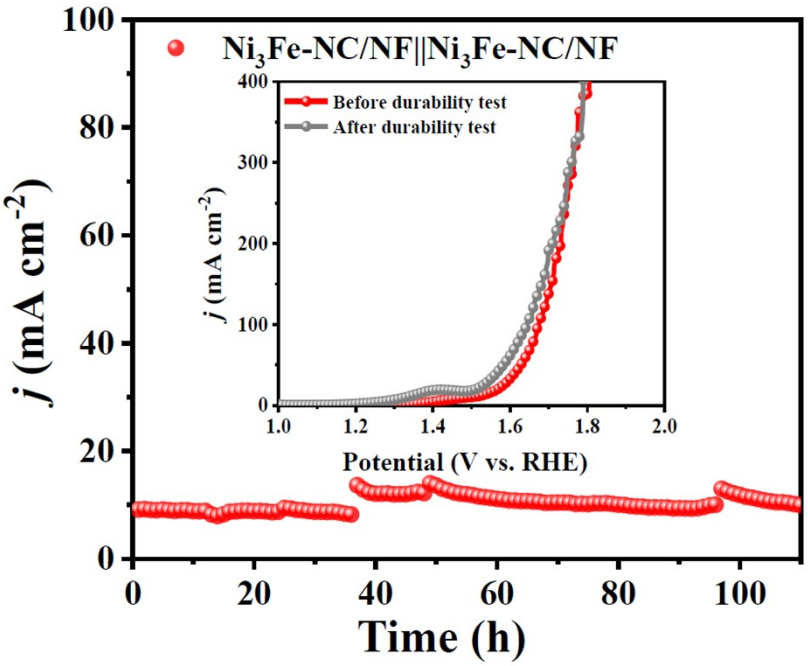

Fig. S24 Chronoamperometry test of Ni_3Fe-NC/NF||Ni_3Fe-NC/NF at the potential of 1.49V in 1 M KOH solution. Inset image shows the LSV polarization curves of Ni_3Fe-NC/NF||Ni_3Fe-NC/NF before and after long-term stability test.

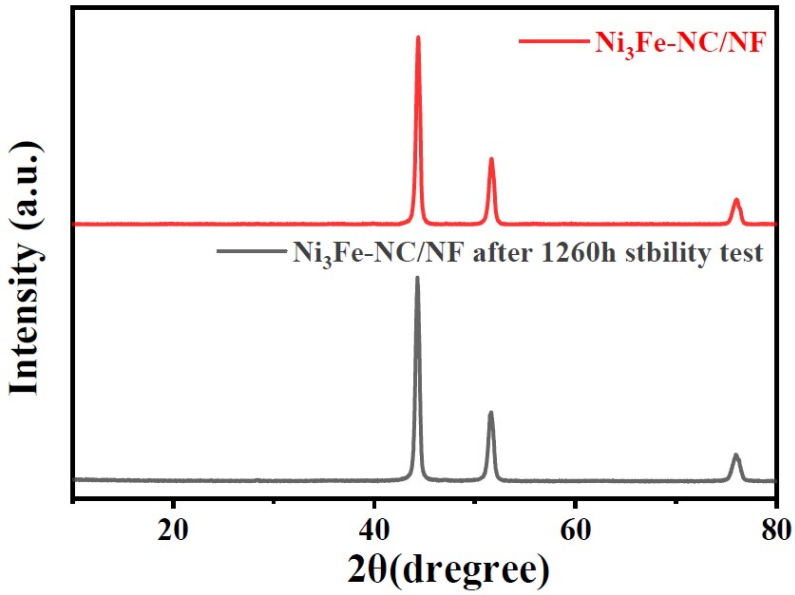

Fig. S25 XRD patterns of Ni_3Fe-NC/NF and the sample collected after 1260 h stability test for all water splitting.

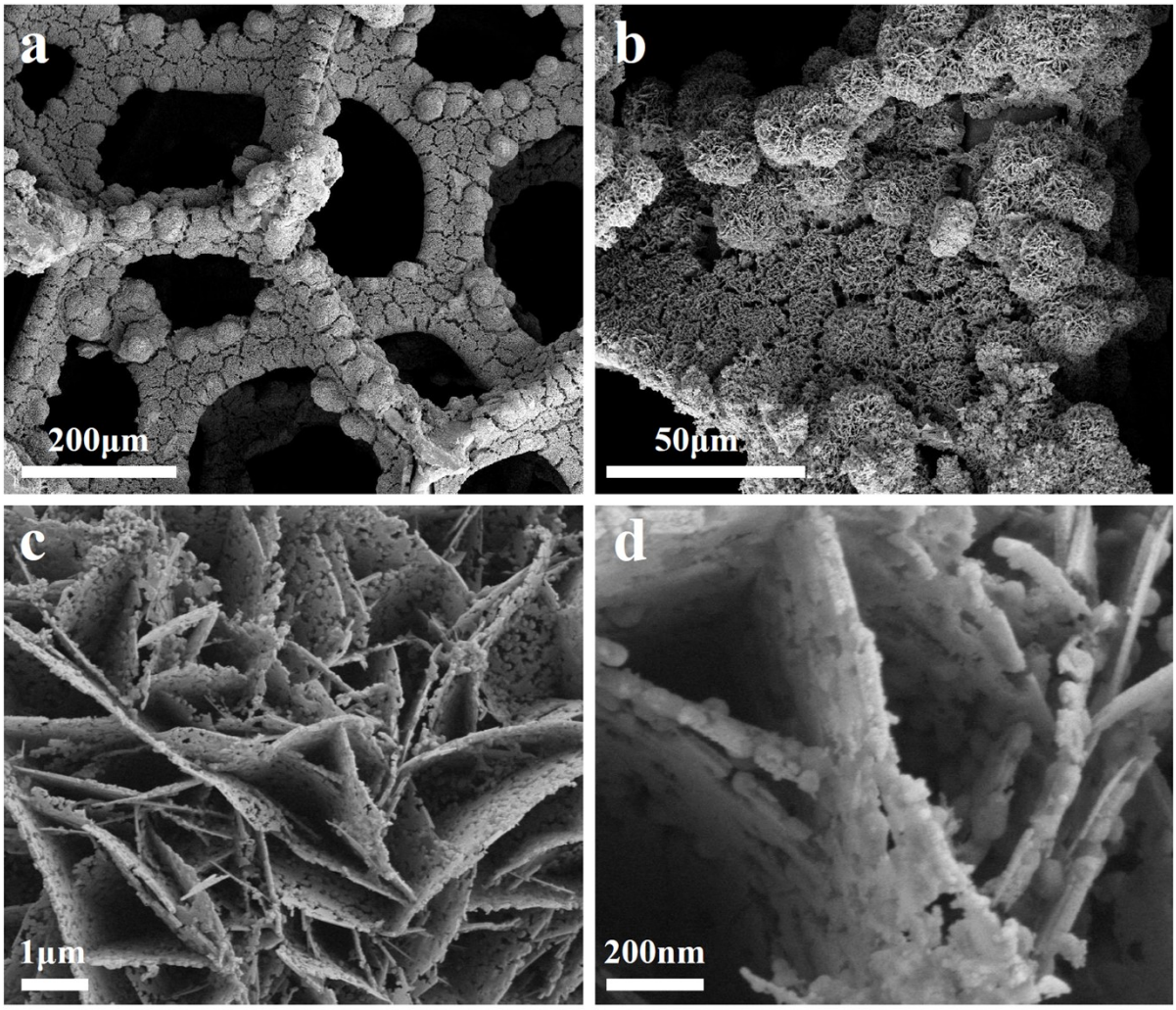

Fig. S26 (a-d) SEM images of Ni_3Fe-NC/NF after 1260 h stability test for all water splitting.

Table S1. Comparison of OER and HER performance of Ni_3Fe-NC/NF in 1M KOH with other reported bifunctional electrocatalysts.

Samples	OER η_{10} (mV)	HER η_{10} (mV)	Ref.no
fcc-Ni_3Fe/C	201	70	*Adv. Funct.Mater.*, 2021, **32**, 2109709
Ni_2Fe@NC	237	198	*Electrochim. Acta*, 2021, **389**, 138785
NF-Na-Fe-Pt	261	31	*Appl. Catal. B,* 2021, **297**, 120395
CS-NFO@PNC-700	217	200	*Appl. Catal. B*, 2022, **300**, 120752
CoP@FeCoP/NC	238	141	*Chem. Eng. J.*, 2021, **403**, 120752
Ni_3FeN/r-Go	270	94	*ACS Nano*, 2018, **12**, 245-253
NiFeOP	310	209	*ACS Sustain. Chem. Eng.*, 2021, **9**, 9436-9443
$NiCo_2S_4$	243	80	*Adv. Funct. Mater.*, 2019, **29**, 1807031

NiFe-LDH@NiCu	218	66	*Adv. Mater.*, 2019, **31**, e1806769
Ni_3FeN/Ni_3Fe	250	125	*J. Mater. Chem. A*, 2021, **9**, 4036-4043
NiFe@OCC	281	256	*ChemElectroChem*, 2019, **6**, 2497-2502
NiFe(II,III)-LDH	220	120	*Small*, 2019, **15**, e1902551
$NiO/NiFe_2O_4$	279	282	*Small*, 2021, **17**, e2103501
Cu_3P-Cu_2O/NPC	286	138	*Chem. Eng. J.*, 2022, **427**, 130946
10: MoCo-VS_2/CC	248	160	*J. Mater. Chem. A*, 2022, **10**, 9067-9079
Mo_2NiB_2	280	160	*Small*, 2022, **18**, e2104303
Ni_3Fe-NC/NF	**203**	**98**	**This work**

Table S2. Comparison of the cell voltage of overall water-splitting for Ni_3Fe-NC/NF in 1M KOH and other bifunctional electrocatalysts.

Samples	**E (V)@ 10 mA cm^{-2}**	**Ref.no**
hcp-Ni_3Fe/C	1.54	*Adv. Funct.Mater.*, 2021, **32**, 2109709
Ni_2Fe@NC	1.81	*Electrochim. Acta*, 2021, **389**, 138785
NF-Na-Fe-Pt	1.56	*Appl. Catal. B,* 2021, **297**, 120395
CS-NFO@PNC-700	1.66	*Appl. Catal. B*, 2022, **300**, 120752
CoP@FeCoP/NC	1.68	*Chem. Eng. J.*, 2021, **403**, 120752
Ni_3FeN/r-Go	1.6	*ACS Nano*, 2018, **12**, 245-253
NiFeOP	1.69	*ACS Sustain. Chem. Eng.*, 2021, **9**, 9436-9443
$NiCo_2S_4$	1.58	*Adv. Funct. Mater.*, 2019, **29**, 1807031
Ni_3FeN/Ni_3Fe	1.61	*J. Mater. Chem. A*, 2021, **9**, 4036-4043
NiFe@OCC	1.7	*ChemElectroChem*, 2019, **6**, 2497-2502
NiFe(II,III)-LDH	1.54	*Small*, 2019, **15**, e1902551
Cu_3P-Cu_2O/NPC	1.57	*Chem. Eng. J.*, 2022, **427**, 130946
10: MoCo-VS_2/CC	1.54	*J. Mater. Chem. A*, 2022, **10**, 9067-9079
Mo_2NiB_2	1.57	*Small*, 2022, **18**, e2104303
CuNi@NiFeCu/CP	1.51	*Appl. Catal. B*, 2021, **298**, 120600
NiFeOx(OH)y@MoS_2/rGo	1.57	*Chem. Eng. J.*, 2020, **397**, 125454
NiFeP@NC/Ni_2P	1.57	*Small*, 2021, **17**, e2006860
Ni_3Fe-NC/NF	**1.49**	**This work**

Table S3. Comparison of the stability of overall water splitting for Ni_3Fe-NC/NF in 1M KOH with other reported bifunctional catalysts.

Samples	***j***	**Tim**	**Ref.no**

	(mA cm^{-2})	e (h)	
hcp-Ni_3Fe/C	10	36	*Adv. Funct.Mater.*, 2021, **32**, 2109709
NF-Na-Fe-Pt	10	12	*Appl. Catal. B,* 2021, **297**, 120395
Ni_3FeN/r-Go	10	100	*ACS Nano*, 2018, **12**, 245-253
d-Ni_3FeN/Ni_3Fe	70	90	*J. Mater. Chem. A*, 2021, **9**, 4036-4043
CuNi@NiFeCu/CP	80	50	*Appl. Catal. B*, 2021, **298**, 120600
NiFeOx(OH)y@MoS_2/rGo	20	12	*Chem. Eng. J.*, 2020, **397**, 125454
NiFeRh-LDH	100	150	*Appl. Catal. B*, 2021, **284**, 119740
Ni_3N-Co_3N/C	10	168	*Appl. Catal. B*, 2021, **297**, 120461
FNP	10	80	*Chem. Eng. J.*, 2020, **390**, 124515
CuO@CoZn-LDH/CF	10	48	*Chem. Eng. J.*, 2021, **414**, 128809
VCoCox@NF	10	70	*Chem. Eng. J.*, 2022, **430**, 132623
Fe/Mo_2C-NCS	100	24	*Chem. Eng. J.*, 2022, **431**, 134126
CoFe-250	60	24	*Chem. Eng. J.*, 2022, **432**, 134275
ZCNP/NF	20	200	*Adv. Funct. Mater.*, 2019, **29**, 1808889
a-CoMoPx/CF	100	100	*Adv. Funct. Mater.*, 2020, **30**, 2003889
Ni_3Fe-NC/NF	**160**	**1260**	**This work**